Electronic Transactions on Numerical Analysis.
Volume 65, pp. 140–155, 2026.

ISSN 1068–9613.
DOI: 10.1553/etna_vol65s140

ETNA
Kent State University and
Johann Radon Institute (RICAM)

UNIFORM ASYMPTOTIC APPROXIMATION AND NUMERICAL EVALUATION OF THE REVERSE GENERALIZED BESSEL POLYNOMIAL ZEROS*

T. M. DUNSTER†, A. GIL‡, D. RUIZ-ANTOLIN‡, AND J. SEGURA§

Abstract. Uniform asymptotic expansions are derived for the zeros of the reverse generalized Bessel polynomials of large degree n and real parameter a. It is assumed that $-\Delta_1 n + \frac{3}{2} \le a \le \Delta_2 n$ for fixed arbitrary $\Delta_1 \in (0,1)$ and bounded positive Δ_2. For this parameter range, at most one of the zeros is real, with the rest being complex conjugates. The new expansions are uniformly valid for all the zeros and are shown to be highly accurate for moderate or large values of n. They are consequently used as initial values in a very efficient numerical algorithm designed to obtain the remaining complex zeros using a Taylor series.

Key words. asymptotic expansions, turning point theory, WKB theory, Bessel polynomials, numerical algorithms

AMS subject classifications. 34E05, 33C10, 34M60, 34E20

1. Introduction.

The generalized Bessel polynomials are defined by

$$y_n(z;a) = \sum_{k=0}^{n} \binom{n}{k} (n+a-1)_k \left(\tfrac{1}{2}z\right)^k, \qquad -a \notin \mathbb{N},$$

where $(\alpha)_k = \Gamma(\alpha+k)/\Gamma(\alpha)$, $k \ge 0$, is Pochhammer's symbol. These polynomials have been explored for nearly a century, with earlier studies of the non-generalized case dating back to the work of Bochner [1] and Romanowsky [20]. It was in the seminal paper by Krall and Frink [15] that the term "Bessel polynomials" was coined and their connection to the problem of traveling spherical waves was established. A thorough study of the properties satisfied by these polynomials, as well as an extensive list of references, can be found in Grosswald's volume [12].

On the other hand, the zeros of Bessel polynomials arise in a number of applications in applied mathematics [14] and engineering; see, for example, [2, 11, 13, 17]. The first analytic approach to the study of the zeros of generalized Bessel polynomials, including an investigation of the domains in which the zeros lie, was given in [4, 5]. Subsequent studies on this topic include, for example, [3]. A related study on the zero distribution of Laguerre polynomials with negative parameter (which are closely connected to reverse generalized Bessel polynomials), carried out using a Riemann–Hilbert formulation, can be found in [16]. With regard to the computation of the zeros of generalized Bessel polynomials, an earlier work addressing this problem is [19]. In addition, [21] presents a general method for computing complex zeros of special functions, one of the cases considered being the zeros of reverse generalized Bessel polynomials.

In this paper, we derive uniform asymptotic expansions for these zeros as $n \to \infty$, which are uniformly valid for *all* the zeros and for $-\Delta_1 n + \frac{3}{2} \le a \le \Delta_2 n$, with fixed arbitrary $\Delta_1 \in (0,1)$ and bounded positive Δ_2. These expansions are considerably more powerful than

*Received December 7, 2025. Accepted February 20, 2026. Published online on May 11, 2026. Recommended by Dario Bini. Financial support from Ministerio de Ciencia e Innovación projects PID2021-127252NB-I00 and PID2024-159583NB-I00 (MICIU/ AEI / 10.13039/501100011033 / FEDER, UE) are acknowledged.

†Department of Mathematics and Statistics, San Diego State University, 5500 Campanile Drive, San Diego, CA 92182, USA (mdunster@sdsu.edu).

‡Corresponding author: Amparo Gil. Departamento de Matemática Aplicada y CC. de la Computación, Universidad de Cantabria, 39005-Santander, Spain ({amparo.gil, diego.ruizantolin}@unican.es).

§Departamento de Matemáticas, Estadística y Computación, Universidad de Cantabria, 39005-Santander, Spain (javier.segura@unican.es).

ETNA
Kent State University and
Johann Radon Institute (RICAM)

existing results—which focus on the regions in which the zeros lie rather than on asymptotic expansions—since they are uniformly valid for large n and for both small and large values of $|a|$, including those close to the turning point. They are derived in Section 3, employing certain coefficients presented in Section 2, and are shown to be highly accurate for moderate or large values of n. Moreover, they can be used as starting values in a new, highly efficient numerical algorithm developed in Section 4, which is designed to compute the remaining complex zeros using a Taylor series.

It is important to note that the method presented in [19] for computing the zeros of generalized Bessel polynomials requires good initial approximations and is computationally expensive, as we will show later. In contrast, our algorithm is very efficient even when a large number of zeros are required. Furthermore, the use of the Taylor series avoids the explicit evaluation of the function; since only the zeros are needed, the overall normalization is irrelevant, which simplifies the computation.

In our analysis, following [7, 9, 10], we find it more convenient to consider the reverse Bessel polynomials, which are given by

$$\theta_n(z;a) = z^n y_n(z^{-1};a).$$

Then, following [7, (2.3), (2.4)], define the scaled function

$$w_n^{(0)}(z;a) = 2^{-n-a+1} z^{1-n-a/2} e^{-z} \theta_n(z;a), \tag{1.1}$$

which satisfies the differential equation

$$\frac{d^2w}{dz^2} = \left\{1 + \frac{a-2}{z} + \frac{(2n+a)(2n+a-2)}{4z^2}\right\} w. \tag{1.2}$$

It has a regular singularity at $z=0$ and an irregular singularity at infinity. The significance of $w_n^{(0)}(z;a)$ is that it is the solution that is recessive at infinity in the right half-plane since

$$w_n^{(0)}(z;a) = 2^{-n-a+1} z^{1-a/2} e^{-z} \left\{1 + \mathcal{O}(z^{-1})\right\} \qquad (z \to \infty).$$

As in [9], we also use two numerically satisfactory companion solutions of (1.2), namely

$$w_n^{(1)}(z;a) = (-1)^{n+1} z^{n+a/2} e^{-z} V(n+a-1, 2n+a, 2z)$$

and

$$w_n^{(-1)}(z;a) = z^{n+a/2} e^{-z} M(n+a-1, 2n+a, 2z), \tag{1.3}$$

where $V(a,b,z)$ and $M(a,b,z)$ are certain confluent hypergeometric functions; see [18, pp. 255–256]. The functions $w_n^{(1)}(z;a)$ and $w_n^{(-1)}(z;a)$ are recessive at $z=\infty$ in the left half-plane $|\arg(-z)| < \frac{1}{2}\pi$ and at $z=0$, respectively. This follows from the limiting behavior

$$w_n^{(1)}(z;a) = 2^{-n-1} z^{(a/2)-1} e^{z} \left\{1 + \mathcal{O}(z^{-1})\right\} \qquad \left(z \to \infty, |\arg(-z)| \le \tfrac{3}{2}\pi - \delta\right),$$

where δ is an arbitrarily small positive constant, and

$$w_n^{(-1)}(z;a) = \frac{z^{n+a/2}}{\Gamma(2n+a)} \left\{1 + \mathcal{O}(z)\right\} \qquad (z \to 0).$$

ETNA
Kent State University and
Johann Radon Institute (RICAM)

2. Liouville–Green coefficients. We define

$$u = n + \frac{1}{2}, \qquad \alpha = \frac{a-2}{u}.$$

Then the differential equation (1.2) can be rewritten in the form

$$\frac{d^2w}{dz^2} = \left\{u^2 f(\alpha, z) + g(z)\right\} w, \tag{2.1}$$

where

$$f(\alpha, z) = \frac{\left(z + \frac{1}{2}\alpha\right)^2 + 1 + \alpha}{z^2}, \qquad g(z) = -\frac{1}{4z^2}. \tag{2.2}$$

On factoring, we note that

$$f(\alpha, z) = \frac{(z - z_1)(z - z_2)}{z^2},$$

where

$$z_{1,2}(\alpha) = \pm i\sigma - \tfrac{1}{2}\alpha,$$

in which

$$\sigma = \sqrt{1 + \alpha}. \tag{2.3}$$

Thus, for large u, (2.1) has turning points at $z = z_{1,2}$. Following [9], we assume

$$-1 < -1 + \delta \le \alpha \le \alpha_1 < \infty, \tag{2.4}$$

and, as such, the two turning points are bounded complex conjugates, bounded away from each other and from the pole at $z = 0$.

In our expansions for the zeros, we use a Liouville–Green (LG) variable ξ, along with the Liouville variable ζ, which appears in turning-point expansions; see [18, Chapters 10–11]. These are given in the present case by

$$\begin{aligned} \frac{2}{3}\zeta^{3/2} = \xi &= \int_{z_1(\alpha)}^{z} f^{1/2}(\alpha, t)\, dt \\ &= Z - \left(1 + \tfrac{1}{2}\alpha\right) \ln\left\{\frac{4Z + 2\alpha(Z + z + 2) + 4 + \alpha^2}{z}\right\} \\ &\quad + \tfrac{1}{2}\alpha \ln(2Z + 2z + \alpha) + \tfrac{1}{2}\ln(1 + \alpha) \\ &\quad + \left(2 + \tfrac{1}{2}\alpha\right)\ln(2) - \tfrac{1}{2}(1 + \alpha)\pi i, \end{aligned} \tag{2.5}$$

where

$$Z = \{(z - z_1)(z - z_2)\}^{1/2} = \left\{\left(z + \tfrac{1}{2}\alpha\right)^2 + 1 + \alpha\right\}^{1/2}. \tag{2.6}$$

The branch of the square root in (2.6) is chosen so that $Z > 0$ for $z > 0$ and $Z < 0$ for $z < 0$, with Z being continuous throughout the upper half of the complex z-plane, except along a branch cut connecting $z = 0$ to the turning point z_1, where the imaginary part of ξ vanishes. This cut traces the so-called anti-Stokes line. With this choice, we have $Z \sim z$ as

ETNA
Kent State University and
Johann Radon Institute (RICAM)

$z \to \infty$ in the upper half-plane ($\Im(z) \geq 0$). Furthermore, principal branches are used for the logarithmic terms appearing in (2.5). A detailed description of the associated conformal mapping is provided in [9].

The following coefficients appearing in LG expansions were constructed in [9], and we shall use them here. First, let $\phi \in \mathbb{C}$ be defined by

$$\sin(\phi) = \frac{\sigma}{Z}, \tag{2.7}$$

and hence, from (2.6),

$$\cos(\phi) = \frac{z + \frac{1}{2}\alpha}{Z}. \tag{2.8}$$

The functions $\sin(\phi)$ and $\cos(\phi)$ are both positive when $z > 0$, and they extend continuously throughout the upper half-plane $\Re(z) \geq 0$, except along the branch cut extending from $z = 0$ to the turning point z_1, i.e., along the anti-Stokes line as described above. In particular, $\cos(\phi)$ is positive for all z in the interval $(-\infty, -\frac{1}{2}\alpha)$ and approaches 1 as $z \to \infty$ along any ray in the upper half-plane. Also observe that, by combining (2.7) and (2.8), one obtains the relation

$$z = \sigma\, \cot(\phi) - \tfrac{1}{2}\alpha. \tag{2.9}$$

With these definitions, the LG coefficients that we shall use are given by

$$\mathrm{E}_1(\alpha, \phi) = \frac{\sin(\phi)\left\{5\cos^2(\phi) - 2\right\}}{24\,\sigma} + \frac{\alpha\left\{\cos(\phi)\left(5\cos^2(\phi) - 6\right) + 1\right\}}{48(1+\alpha)}, \tag{2.10}$$

$$\begin{aligned}\mathrm{E}_2(\alpha, \phi) = {} & \frac{\alpha\cos(\phi)\sin^3(\phi)\left\{3 - 5\cos^2(\phi)\right\}}{16\,(1+\alpha)^{3/2}} \\ & + \frac{\sin^2(\phi)}{64(1+\alpha)^2}\Big\{5\left(4 - \alpha^2 + 4\alpha\right)\cos^4(\phi) \\ & \qquad + (7\alpha^2 - 16\alpha - 16)\cos^2(\phi) - 2\alpha^2\Big\},\end{aligned} \tag{2.11}$$

and, for $s = 2, 3, 4, \ldots$,

$$\mathrm{E}_{s+1}(\alpha, \phi) = G(\alpha, \phi)\frac{\partial \mathrm{E}_s(\alpha, \phi)}{\partial \phi} + \int_0^{\phi} G(\alpha, \varphi) \sum_{j=1}^{s-1} \frac{\partial \mathrm{E}_j(\alpha, \varphi)}{\partial \varphi} \frac{\partial \mathrm{E}_{s-j}(\alpha, \varphi)}{\partial \varphi} d\varphi, \tag{2.12}$$

where

$$G(\alpha, \phi) = -\frac{1}{2}\frac{d\phi}{d\xi} = \frac{\cos(\phi)\sin^2(\phi)}{2\sigma} - \frac{\alpha\sin^3(\phi)}{4(1+\alpha)}. \tag{2.13}$$

The lower integration limits in (2.12) are chosen for convenience so that $\mathrm{E}_s(\alpha, 0) = 0$, which means that they vanish as $z \to \infty$.

Next, let

$$a_1 = a_2 = \tfrac{5}{72}, \qquad \tilde{a}_1 = \tilde{a}_2 = -\tfrac{7}{72},$$

with subsequent terms a_s and $\tilde{a}_s$ satisfying the same recursion formula, namely

$$a_{s+1} = \frac{1}{2}(s+1)\,a_s + \frac{1}{2}\sum_{j=1}^{s-1} a_j a_{s-j}, \qquad s = 2, 3, 4, \ldots$$

ETNA
Kent State University and
Johann Radon Institute (RICAM)

Further, define

$$\tilde{\mathcal{E}}_s(a,z) = \mathrm{E}_s(\alpha,\phi) + (-1)^s \frac{\tilde{a}_s}{s\xi^s} \tag{2.14}$$

and

$$\mathcal{E}_s(a,z) = \mathrm{E}_s(\alpha,\phi) + (-1)^s \frac{a_s}{s\xi^s}. \tag{2.15}$$

Also, let the sequence $d_{2s+1}(\alpha)$, $s = 0, 1, 2, \ldots$, be given by

$$\frac{1}{2}\Bigg[u\alpha(\ln(u)-1) + u(1+\alpha)\ln(1+\alpha) + \ln\left\{\Gamma\left(u+\frac{1}{2}\right)\right\} - \ln\left\{\Gamma\left(u+u\alpha+\frac{1}{2}\right)\right\}\Bigg] \sim \sum_{s=0}^{\infty} \frac{d_{2s+1}(\alpha)}{u^{2s+1}} \quad (u\to\infty).$$

The first four terms are given by

$$d_1(\alpha) = -\frac{\alpha}{48(1+\alpha)}, \tag{2.16}$$

$$d_3(\alpha) = \frac{7\alpha\left(3+3\alpha+\alpha^2\right)}{5760(1+\alpha)^3}, \tag{2.17}$$

$$d_5(\alpha) = -\frac{31\alpha\left(5+10\alpha+10\alpha^2+5\alpha^3+\alpha^4\right)}{80640(1+\alpha)^5}, \tag{2.18}$$

and

$$d_7(\alpha) = \frac{127\alpha\left(7+21\alpha+35\alpha^2+35\alpha^3+21\alpha^4+7\alpha^5+\alpha^6\right)}{430080(1+\alpha)^7}. \tag{2.19}$$

Then, from [9, Theorem 3.2], we have the following:

THEOREM 2.1.

$$\theta_n(uz;a) = \frac{u^{1/6}}{e^{(u+a+2)\pi i/2}} \left\{\frac{2^a\pi n!}{\Gamma(n+a-1)}\right\}^{1/2} \left\{\frac{\zeta}{f(a,z)}\right\}^{1/4} (uz)^{n+\frac{1}{2}a-1} e^{uz} \times \left\{\mathrm{Ai}\left(u^{2/3}\zeta\right) A(u,a,z) + \mathrm{Ai}'\left(u^{2/3}\zeta\right) B(u,a,z)\right\},$$

where

$$A(u,a,z) \sim \exp\left\{\sum_{s=1}^{\infty} \frac{\tilde{\mathcal{E}}_{2s}(a,z)}{u^{2s}}\right\} \cosh\left\{\sum_{s=0}^{\infty} \frac{\tilde{\mathcal{E}}_{2s+1}(a,z) + d_{2s+1}(\alpha)}{u^{2s+1}}\right\},$$

$$B(u,a,z) \sim \frac{1}{u^{1/3}\zeta^{1/2}} \exp\left\{\sum_{s=1}^{\infty} \frac{\mathcal{E}_{2s}(a,z)}{u^{2s}}\right\} \sinh\left\{\sum_{s=0}^{\infty} \frac{\mathcal{E}_{2s+1}(a,z) + d_{2s+1}(\alpha)}{u^{2s+1}}\right\},$$

as $u\to\infty$, *uniformly for* $0 \le \arg(z) \le \pi$, *with* $|z-z_1| \ge \delta > 0$, *under the condition* (2.4). See [9, Remark 1] for how these expansions can be extended to $|z-z_1| \le \delta$.

From [9, Lemma 3.1], we have an important result that is required in the next section:

LEMMA 2.2. *Each* $(z-z_1)^{1/2}\{\mathrm{E}_{2s+1}(\alpha,\phi) + d_{2s+1}(\alpha)\}$, $s = 0, 1, 2, \ldots$, *regarded as a function of* z, *is meromorphic at* $z = z_1$.

ETNA
Kent State University and
Johann Radon Institute (RICAM)

3. Uniform asymptotic expansions for the zeros. We derive asymptotic expansions for the complex zeros of $\theta_n(t;a)$ for large n, which are uniformly valid for unrestricted complex t, subject to (2.4). To do so, we use the method in [8]. We begin by defining a function $\mathcal{Z}(u,a,z)$ and a coefficient $l_n(a)$ by the pair of equations

$$(-1)^n \frac{e^{a\pi i}}{n!} w_n^{(0)}(uz;a) = e^{-\pi i/3} l_n(a) \left\{ \frac{\partial \mathcal{Z}(u,a,z)}{\partial z} \right\}^{-1/2} \mathrm{Ai}\left(u^{2/3}\mathcal{Z}(u,a,z)\right), \tag{3.1}$$

$$\frac{1}{\Gamma(n+a-1)} w_n^{(1)}(uz;a) = l_n(a) \left\{ \frac{\partial \mathcal{Z}(u,a,z)}{\partial z} \right\}^{-1/2} \mathrm{Ai}_1\left(u^{2/3}\mathcal{Z}(u,a,z)\right). \tag{3.2}$$

The factor $\{\partial \mathcal{Z}(u,a,z)/\partial z\}^{-1/2}$, along with Airy's equation [6, (9.2.1)], ensures that both functions on the right-hand side of this pair of equations satisfy a second-order linear differential equation (with independent variable z) that has no first-derivative term, which matches the same property of the functions on the left-hand side of these equations, namely the differential equation (2.1).

Now, from [6, (9.2.12)],

$$\mathrm{Ai}(z) = e^{\pi i/3}\mathrm{Ai}_1(z) + e^{-\pi i/3}\mathrm{Ai}_{-1}(z),$$

and hence, from the connection formula [7, (2.13)]

$$w_n^{(-1)}(t;a) = (-1)^{n+1}\frac{e^{a\pi i}}{n!} w_n^{(0)}(t;a) + \frac{1}{\Gamma(n+a-1)} w_n^{(1)}(t;a), \tag{3.3}$$

we have

$$w_n^{(-1)}(uz;a) = e^{\pi i/3} l_n(a) \left\{ \frac{\partial \mathcal{Z}(u,a,z)}{\partial z} \right\}^{-1/2} \mathrm{Ai}_{-1}\left(u^{2/3}\mathcal{Z}(u,a,z)\right). \tag{3.4}$$

Moreover, $\zeta \to \infty$ as $z \to 0$ or $z \to \pm\infty$; in these cases, $Z \sim \zeta$; see [8]. The fundamental property of (3.1), (3.2), (3.3) is that both functions in each identity are recessive at the same singularities, namely, $z = -\infty, +\infty, 0$, respectively.

In studying the zeros, we do not require the constant $l_n(a)$, but for completeness, we note that it can be determined as follows: from (1.1), (1.3), and [6, (13.2.34)],

$$\mathcal{W}\left\{ w_n^{(0)}(t;a), w_n^{(-1)}(t;a) \right\} = \frac{2^{1-2n-a}}{\Gamma(n+a-1)}. \tag{3.5}$$

Thus, from (3.1), (3.4), (3.5), and [6, (9.2.8)],

$$l_n(a) = \frac{e^{5\pi i/6} e^{(u+a)\pi i/2} u^{1/6}}{2^{n-1}} \left\{ \frac{\pi}{2^a n! \Gamma(n+a-1)} \right\}^{1/2}.$$

We focus on (3.1) (recalling the definition (1.1)). Now, from [8, Theorem 2.2], we have

$$\mathcal{Z}(u,a,z) \sim \zeta + \sum_{s=1}^{\infty} \frac{\Upsilon_s(a,z)}{u^{2s}} \qquad (u \to \infty), \tag{3.6}$$

where each $\Upsilon_s(a,z)$ is analytic at the turning point $z = z_1$. This expansion is uniformly valid in an unbounded domain that includes the upper half-plane $0 \le \arg(z) \le \pi$. Thus, we shall use it to approximate all the zeros of $\theta_n(t;a)$ (where $t = uz$) with nonnegative imaginary part, while those lying in the lower half-plane are simply the conjugates of these.

ETNA
Kent State University and
Johann Radon Institute (RICAM)

The coefficients $\Upsilon_s(a,z)$ are given by [8, Theorem 2.2], with $\hat{E}_{2s+1}(z)$ replaced by $\mathrm{E}_{2s+1}(\alpha,\phi)+d_{2s+1}(\alpha)$ $(s=0,1,2,\ldots)$. The inclusion of the constants $d_{2s+1}(\alpha)$ is needed to ensure the required property stated in the theorem. From [8, (2.28), (2.40)–(2.42)], the first four coefficients in the series in (3.6) are given by

$$\Upsilon_1=\frac{3\xi(\mathrm{E}_1+d_1)}{2\zeta^2}-\frac{5}{48\zeta^2}, \tag{3.7}$$

$$\Upsilon_2=-\frac{\Upsilon_1^2}{4\zeta}+\frac{5\Upsilon_1}{32\zeta^3}+\frac{3\xi(\mathrm{E}_3+d_3)}{2\zeta^2}-\frac{1105}{9216\zeta^5}, \tag{3.8}$$

$$\Upsilon_3=-\frac{\Upsilon_1\Upsilon_2}{2\zeta}+\frac{\Upsilon_1^3}{24\zeta^2}-\frac{25\Upsilon_1^2}{128\zeta^4}+\frac{5\Upsilon_2}{32\zeta^3}+\frac{1105\Upsilon_1}{2048\zeta^6}+\frac{3\xi(\mathrm{E}_5+d_5)}{2\zeta^2}-\frac{82825}{98304\zeta^8}, \tag{3.9}$$

and

$$\begin{aligned}\Upsilon_4=&-\frac{\Upsilon_1^4}{64\zeta^3}+\frac{\Upsilon_1^2\Upsilon_2}{8\zeta^2}+\frac{175\Upsilon_1^3}{768\zeta^5}-\frac{\Upsilon_1\Upsilon_3}{2\zeta}-\frac{25\Upsilon_1\Upsilon_2}{64\zeta^4}-\frac{\Upsilon_2^2}{4\zeta}\\&-\frac{12155\Upsilon_1^2}{8192\zeta^7}+\frac{5\Upsilon_3}{32\zeta^3}+\frac{1105\Upsilon_2}{2048\zeta^6}+\frac{414125\Upsilon_1}{65536\zeta^9}\\&+\frac{3\xi(\mathrm{E}_7+d_7)}{2\zeta^2}-\frac{1282031525}{88080384\zeta^{11}},\end{aligned} \tag{3.10}$$

with the subsequent ones given in [8, Theorem 2.2].

From [8, Theorem 3.1], we obtain the following uniform asymptotic expansion for the zeros of $\theta_n(t;a)$:

PROPOSITION 3.1. *Let $t_m(u,a)$ be the complex zeros of $\theta_n(t;a)$ in the upper half-plane $\Re(t)\geq 0$, so that*

$$\theta_n(t_m(u,a);a)=0 \qquad (m=1,2,3,\ldots,\lfloor (n+1)/2\rfloor).$$

Then there exist coefficients $\tau_{m,s}(\alpha)$ $(s=0,1,2,\ldots)$ such that

$$t_m(u,a)\sim u\sum_{s=0}^{\infty}\frac{\tau_{m,s}(\alpha)}{u^{2s}}, \tag{3.11}$$

as $u\to\infty$, uniformly for $m=1,2,3,\ldots$

To determine the coefficients, we have, from (1.1), (3.1), that the zeros satisfy the implicit equation

$$\mathcal{Z}(u,a,u^{-1}t_m(u,a))=u^{-2/3}\mathrm{a}_m \qquad (m=1,2,3,\ldots),$$

where $x=\mathrm{a}_m$ is the mth negative zero of $\mathrm{Ai}(x)$ ordered by increasing absolute values.

As a result, the leading term $\tau_{m,0}=\tau_{m,0}(\alpha)$ satisfies the implicit equation

$$\begin{aligned}-\frac{2i}{3u}|\mathrm{a}_m|^{3/2}=&Z_{m,0}+\left(1+\frac{1}{2}\alpha\right)\ln\left\{\frac{\tau_{m,0}}{4Z_{m,0}+2\alpha(Z_{m,0}+\tau_{m,0}+2)+4+\alpha^2}\right\}\\&+\frac{1}{2}\alpha\left\{\ln\left(-2Z_{m,0}-2\tau_{m,0}-\alpha\right)+\pi i\right\}\\&+\frac{1}{2}\ln(1+\alpha)+\left(2+\frac{1}{2}\alpha\right)\ln(2)-\frac{1}{2}(1+\alpha)\pi i,\end{aligned} \tag{3.12}$$

ETNA
Kent State University and
Johann Radon Institute (RICAM)

in which $Z_{m,0} = Z(\tau_{m,0})$, where $Z(z)$ is given by (2.6) with the branch as described below that equation. Thus,

$$Z_{m,0} = Z_{m,0}(\alpha) = -\left\{(\tau_{m,0} - z_1)(\tau_{m,0} - z_2)\right\}^{1/2},$$

which is negative for $-\infty < \tau_{m,0} < 0$, since $z = \tau_{m,0}$ lies to the left of the cut along the anti-Stokes line $\Im(\xi) = 0$ from $z = z_1$ to $z = 0$. For numerical purposes, in (3.12) the second logarithm is expressed in a form that ensures the correct branch for these complex values of $\tau_{m,0}$.

Next, let

$$\zeta_{m,0} = \zeta(\tau_{m,0}) = u^{-2/3}\mathrm{a}_m, \quad \zeta'_{m,0} = \zeta'(\tau_{m,0}), \quad \zeta''_{m,0} = \zeta''(\tau_{m,0}), \quad \ldots,$$

and similarly, for $s = 1, 2, 3, \ldots$, let

$$\Upsilon_{m,s} = \Upsilon_s(\tau_{m,0}), \quad \Upsilon'_{m,s} = \Upsilon'_s(\tau_{m,0}), \quad \Upsilon''_{m,s} = \Upsilon''_s(\tau_{m,0}), \quad \ldots$$

Then we can apply [8, Theorem 3.1] to find the coefficients in (3.11). Having determined $\tau_{m,0}$, the next four coefficients are of the same form as [8, (3.47)–(3.50)] (with the appropriate change of notation). Thus,

$$\tau_{m,1} = -\frac{\Upsilon_{m,1}}{\zeta'_{m,0}}, \tag{3.13}$$

$$\tau_{m,2} = -\frac{1}{2\zeta'_{m,0}}\left\{\tau_{m,1}^2\,\zeta''_{m,0} + 2\tau_{m,1}\,\Upsilon'_{m,1} + 2\Upsilon_{m,2}\right\}, \tag{3.14}$$

$$\begin{aligned}\tau_{m,3} = -\frac{1}{6\zeta'_{m,0}}\Big\{&\tau_{m,1}^3\,\zeta'''_{m,0} + 6\tau_{m,1}\,\tau_{m,2}\,\zeta''_{m,0} + 3\tau_{m,1}^2\,\Upsilon''_{m,1}\\ &+ 6\tau_{m,2}\Upsilon'_{m,1} + 6\tau_{m,1}\Upsilon'_{m,2} + 6\Upsilon_{m,3}\Big\},\end{aligned} \tag{3.15}$$

and[1]

$$\begin{aligned}\tau_{m,4} = -\frac{1}{24\zeta'_{m,0}}\Big\{&\tau_{m,1}^4\,\zeta^{(4)}_{m,0} + 12\tau_{m,1}^2\,\tau_{m,2}\,\zeta'''_{m,0}\\ &+ 24\tau_{m,1}\,\tau_{m,3}\,\zeta''_{m,0} + 12\tau_{m,2}^2\,\zeta''_{m,0}\\ &+ 4\tau_{m,1}^3\,\Upsilon'''_{m,1} + 24\tau_{m,1}\,\tau_{m,2}\,\Upsilon''_{m,1} + 12\tau_{m,1}^2\,\Upsilon''_{m,2}\\ &+ 24\tau_{m,3}\,\Upsilon'_{m,1} + 24\tau_{m,2}\,\Upsilon'_{m,2} + 24\tau_{m,1}\,\Upsilon'_{m,3} + 24\Upsilon_{m,4}\Big\}.\end{aligned} \tag{3.16}$$

These, of course, result in different coefficients from the Bessel-function case, due to the difference here in the variable ζ as well as the Υ coefficients.

3.1. Numerical examples. We now approximate $t_m(u, a)$ by the series (3.11). In order to do so, we require the derivatives with respect to z of ζ, ξ, ϕ, and Υ_s. For the latter, it is convenient to let $\rho = 1/\zeta$. Then, from (2.5),

$$\rho' = -\tfrac{3}{2}\rho^4\xi\xi'. \tag{3.17}$$

[1] There is a misprint in [8, (3.50)].

ETNA
Kent State University and
Johann Radon Institute (RICAM)

For the other derivatives, we use

$$\zeta' = \frac{2\xi'\zeta}{3\xi}, \tag{3.18}$$

$$\xi' = f^{1/2}(a,z) = \frac{\sigma}{z\sin(\phi)}, \tag{3.19}$$

and

$$\phi' = -\frac{\sin^2(\phi)}{\sigma}, \tag{3.20}$$

which follow from (2.2), (2.3), (2.5), (2.7), and (2.9).

We compute the first five terms $\tau_{m,s}$ ($s = 0, 1, 2, 3, 4$) in the expansion (3.11). This is achieved by the following steps:

- For each prescribed n and $m \in \{1, 2, 3, \ldots, \lfloor \frac{1}{2}(n+1) \rfloor\}$, find $\xi = -2i|\mathrm{a}_m|^{3/2}/(3u)$, where $u = n + \frac{1}{2}$, and $\zeta = \zeta_{m,0} = \mathrm{a}_m u^{-2/3}$. Use these values for ξ and ζ below.
- Use (3.12) to numerically evaluate $\tau_{m,0}$. To obtain the correct root we found it efficient to set $\tau_{m,0} = -0.5 + w$ in the equation and then numerically solve for w. Then use $z = \tau_{m,0}$ in what follows.
- Use (2.6), (2.7), (2.8), (2.3), (3.18), (3.19), and (3.20) to compute $\zeta'_{m,0}$, $\zeta''_{m,0}$, $\zeta'''_{m,0}$, and $\zeta^{(4)}_{m,0}$.
- From (2.10), (2.11), (2.12), (2.13), and (3.20), for $z = \tau_{m,0}$, compute E_1 and its first three z-derivatives, E_3 and its first two z-derivatives, E_5 and its z-derivative, and E_7.
- Use (2.14), (2.15), (2.16), (2.17), (2.18), (2.19), (3.7), (3.8), (3.9), (3.10), (3.17), (3.19), (3.20), and the above values to compute, in turn, $\Upsilon_{m,1}$, $\Upsilon'_{m,1}$, $\Upsilon''_{m,1}$, $\Upsilon'''_{m,1}$, $\Upsilon_{m,2}$, $\Upsilon'_{m,2}$, $\Upsilon''_{m,2}$, $\Upsilon_{m,3}$, $\Upsilon'_{m,3}$, and $\Upsilon_{m,4}$.
- Evaluate $\tau_{m,s}$, for $s = 1, 2, 3, 4$, in turn from (3.13), (3.14), (3.15), and (3.16).

Numerical examples of the approximations t_m obtained using the scheme described above are presented in Tables 3.1–3.2 for $a = 1.01$ and 20.2, respectively, and different values of n and m. The approximations, implemented in Maple[2], are compared with the values obtained using the numerical algorithm described in [21] (also implemented in Maple). The relative errors from these comparisons are presented in the tables. Relative errors are all close to or less than 10^{-15}.

In the implementation of the numerical algorithm, the reverse generalized Bessel polynomials are evaluated through their relation with the varying Laguerre polynomials [6, § 18.34(i)]

$$\theta_n(z;a) = \left(-\tfrac{1}{2}\right)^n n! L_n^{(1-2n-a)}(2z).$$

Furthermore, Figure 3.1 displays the relative error of the approximations to the zeros for various values of a (with n fixed at 15 and m at 3). It is observed that the relative error decreases as a increases, and the maximum relative error attained is less than 4×10^{-15}.

Notably, equation (3.12) can be solved using Newton's method to obtain the corresponding root. By expressing the equation as $F(w) = 0$, Figure 3.2 illustrates, as an example, a plot of the function $F(w)$ for $a = 1.01$, $m = 10$, and $n = 30$. The root obtained by applying Newton's method is $w = -0.0935299175 + 0.310545771i$, which agrees with the location of the zero of $F(w)$ shown in the figure.

[2]The file can be obtained from https://github.com/AmparoGil/AsympZerosRGBPs.

ETNA
Kent State University and
Johann Radon Institute (RICAM)

TABLE 3.1
Approximations of the zeros of the reverse generalized Bessel polynomials for $a = 1.01$ and different values of n and m.

n, m	t_m	Relative error
15, 1	$-3.1559515225814951808 + 12.586271690843017387i$	1.8×10^{-15}
15, 3	$-6.9360218173803455640 + 8.6292759166638006520i$	6.1×10^{-16}
30, 1	$-4.2425750716206130472 + 27.006358468998877565i$	1.1×10^{-16}
30, 3	$-9.7584463264409865096 + 22.392832031435945931i$	1.3×10^{-16}
30, 10	$-18.102790325129739597 + 9.4722422021510892034i$	7.7×10^{-17}
30, 15	$-19.702854218331257062 + 0.8561127155082006120i$	2.9×10^{-16}
50, 1	$-5.2055266715795128190 + 46.482961682470093754i$	1.9×10^{-17}
50, 3	$-12.181102558122645217 + 41.239145916888100131i$	7.9×10^{-17}
50, 10	$-24.683402130958153499 + 27.225504025486397962i$	1.4×10^{-16}
50, 15	$-29.379559025204265717 + 18.222895815367965462i$	2.2×10^{-16}
50, 25	$-32.962750529211803345 + 0.86074820845854851941i$	6.7×10^{-18}

TABLE 3.2
Approximations of the zeros of the reverse generalized Bessel polynomials for $a = 20.2$ and different values of n and m.

n, m	t_m	Relative error
15, 1	$-12.715856054909203812 + 18.788546633810651464i$	1.1×10^{-15}
15, 3	$-16.514653825298059143 + 12.612556755577648289i$	2.6×10^{-15}
30, 1	$-13.800334806578766149 + 34.380365451162645216i$	3.4×10^{-16}
30, 3	$-19.310221900147056579 + 28.210989284732813206i$	2.8×10^{-16}
30, 10	$-27.717880396627235555 + 11.750965665786499280i$	5.4×10^{-17}
30, 15	$-29.339399892921113584 + 1.0590134228243351098i$	2.8×10^{-16}
50, 1	$-14.766307319696546646 + 54.504885286408130512i$	2.9×10^{-16}
50, 3	$-21.724567399352576652 + 48.087744580616150218i$	6.1×10^{-17}
50, 10	$-34.260698846474016613 + 31.438165321383787957i$	1.6×10^{-16}
50, 15	$-38.989834370513922989 + 20.967450446744804559i$	2.3×10^{-16}
50, 25	$-42.605131456252572254 + 0.98772884689217274560i$	2.6×10^{-18}

4. A numerical algorithm to compute the zeros of $\theta_n(z; a)$. Given that the asymptotic approximations obtained exhibit high accuracy for moderate to large values of n, they can be employed as initial estimates in the numerical algorithm described in [21], devised to compute all the zeros. Within this algorithm, the fundamental components are an iteration function $T_n(a, z)$ and a step function $H_n(a, z)$:

$$T_n(a,z) = z - \frac{1}{\sqrt{\Omega_n(a,z)}} \arctan\left(\frac{\sqrt{\Omega_n(a,z)}\, w_n^{(0)}(z;a)}{\partial w_n^{(0)}(z;a)/\partial z} \right), \tag{4.1}$$

$$H_n(a,z) = z + \frac{\pi}{\sqrt{\Omega_n(a,z)}}, \tag{4.2}$$

ETNA
Kent State University and
Johann Radon Institute (RICAM)

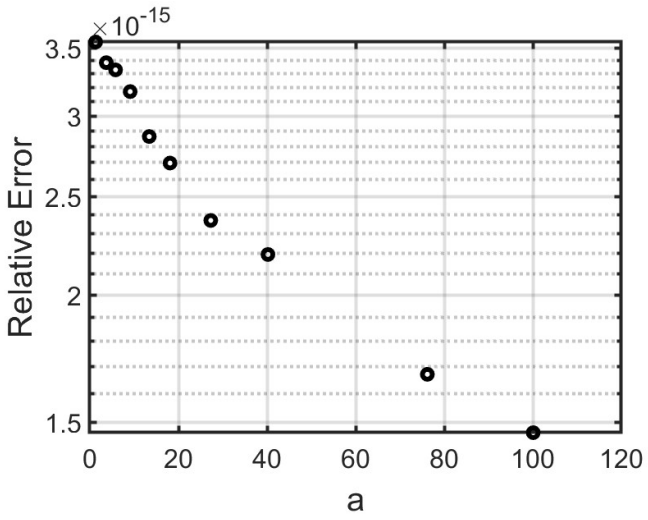

FIG. 3.1. *Relative errors as a function of a (with n fixed at 15 and m at 3).*

where

$$\Omega_n(a,z) = -1 + \frac{2-a}{z} - \left(n+\frac{1}{2}a\right)\left(n+\frac{1}{2}a-1\right)\frac{1}{z^2}.$$

The function $w_n^{(0)}(z;a)$ appearing in (4.1) is related to the reverse generalized Bessel polynomials $\theta_n(z;a)$ by (1.1). It is therefore clear that $w_n^{(0)}(z;a)$ can be used to locate the zeros of $\theta_n(z;a)$. In [10], we discussed the possible use of asymptotic expansions to compute the reverse generalized Bessel polynomials appearing in the iteration function (4.1). However, this is not necessary if accurate approximations are available for the first zero (combined with the use of the Taylor series). This is precisely the strategy we discuss next. The resulting algorithm, which avoids the explicit computation of the function in order to locate its zeros, is both accurate and highly efficient.

We use as a starting point for finding the Taylor series the equation satisfied by $w_n^{(0)}(z;a)$, written in the form

$$Pw_n'' + Q_n w_n = 0,$$

where

$$P = P(z) = z^2, \qquad Q_n = Q_n(a,z) = z^2\Omega_n(a,z).$$

We have $P^{(m)} = Q_n^{(m)} = 0$, for $m > 2$. Then, we obtain for $w_n = w_n^{(0)}(z;a)$

$$\sum_{m=0}^{2}\binom{j}{m}\left\{P^{(m)}w_n^{(j+2-m)} + Q_n^{(m)}w_n^{(j-m)}\right\} = 0,$$

which gives the following recurrence relation for the derivatives:

$$\begin{aligned} &z^2 w_n^{(k+2)} + 2kzw_n^{(k+1)} + \{Q_n + k(k-1)\}\, w_n^{(k)} \\ &\quad - k(2z+a-2)w_n^{(k-1)} - k(k-1)w_n^{(k-2)} = 0 \qquad (k = 2,3,4,\ldots). \end{aligned} \tag{4.3}$$

ETNA
Kent State University and
Johann Radon Institute (RICAM)

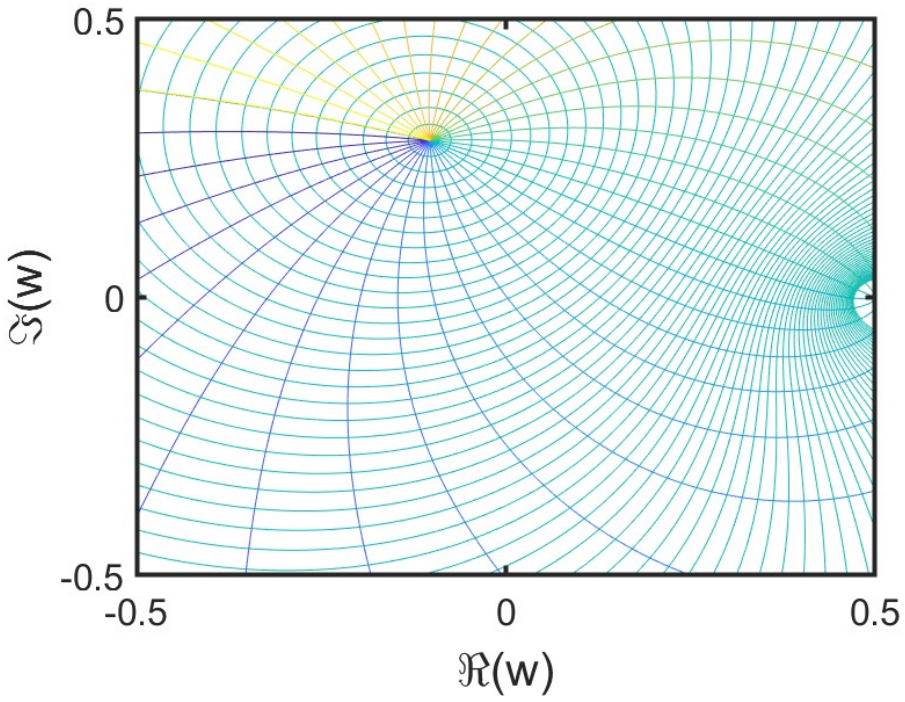

FIG. 3.2. *Plot of the function $F(w)$ for $a = 1.01$, $m = 10$, and $n = 30$.*

This recurrence relation, which is not ill-conditioned as k becomes large, can be used to compute the derivatives appearing in the Taylor series

$$\begin{aligned} w_n(z_{i+1}) &= \sum_{k=0}^{N} w_n^{(k)}(z_i)\frac{h^k}{k!} + \mathcal{O}(h^{N+1}), \\ w_n'(z_{i+1}) &= \sum_{k=0}^{N} w_n^{(k+1)}(z_i)\frac{h^k}{k!} + \mathcal{O}(h^{N+1}). \end{aligned} \tag{4.4}$$

To apply (4.3) in the algorithm step by step, we need $w_n(z_i)$ and $w_n'(z_i)$, which are known from the previous step, and (again suppressing the a-dependence)

$$w_n''(z_i) = -\frac{Q_n(z_i)}{P(z_i)} w_n(z_i),$$

$$w_n'''(z_i) = -\frac{Q_n(z_i)}{P(z_i)} w_n'(z_i) + \left\{ \frac{(2-a)}{z_i^2} - \frac{2\left(n+\frac{1}{2}a\right)\left(n+\frac{1}{2}a-1\right)}{z_i^3} \right\} w_n(z_i).$$

The resulting algorithm works as follows: after a zero z_i has been obtained (using an asymptotic approximation for the first zero), the next zero z_{i+1} is obtained by taking the step $H_n(a,z)$ given in (4.2) and then iterating $T_n(a,z)$ given by (4.1) until convergence is reached. The Taylor series (4.4) are used to calculate the functions $w_n(z)$ and $w_n'(z)$ needed in the iteration function, and the values $w_n(z_i) = 0$ and $w_n'(z_i) = 1$ are used in this computation. A MATLAB implementation of the algorithm can be obtained from GitHub[3].

[3] https://github.com/AmparoGil/NumerZerosRGBPs.

ETNA
Kent State University and
Johann Radon Institute (RICAM)

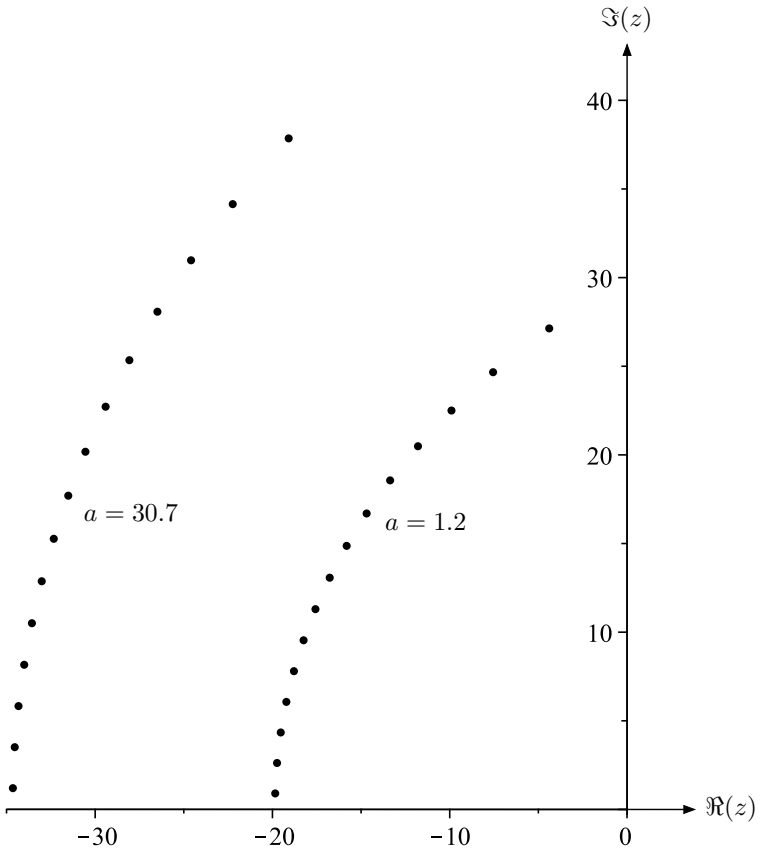

FIG. 4.1. *Zeros in the second quadrant obtained by the numerical algorithm for* $n = 30$ *and* $a = 1.2,\ 30.7$.

In the present implementation and for reasons of computational efficiency, only the first three coefficients of the uniform expansion (3.11) are employed in order to approximate the first zero to be computed (namely, the one with the largest real part in absolute value). The algorithm computes the complex zeros with nonnegative imaginary part (as mentioned before, the remaining complex zeros are simply the complex conjugates of those obtained).

Plots of the zeros of $\theta_n(z;a)$ in the second quadrant obtained by the numerical algorithm are displayed in Figures 4.1–4.2 for $n = 30$, $n = 500$, $a = 1.2$, and $a = 30.7$. The accuracy prescribed for the iterations with $T_n(a,z)$ is $\epsilon = 10^{-12}$, although the precision attained for the zeros is higher when the value of n is sufficiently large, as can be observed in Figure 4.3. The relative errors have been obtained by comparison with the Maple implementation of the numerical algorithm used in Section 3.1. The number of digits was set to 60 in the Maple implementation in order to ensure the correct evaluation of the quotients appearing in the iteration function. It can be observed that, even when a large number of zeros are computed, the relative errors remain well controlled.

Regarding the efficiency of the computations, Table 4.1 presents representative CPU times obtained from the execution of our numerical algorithm for several values of n. CPU times are measured by executing our algorithm in MATLAB R2024b on a Dell Latitude 7410 equipped with 16 GB of RAM and an Intel Core i5–10210U CPU at 1.6 GHz. Notably, increasing from computing 15 zeros ($n = 30$) to 1000 zeros ($n = 2000$) increases the CPU time by only a

ETNA
Kent State University and
Johann Radon Institute (RICAM)

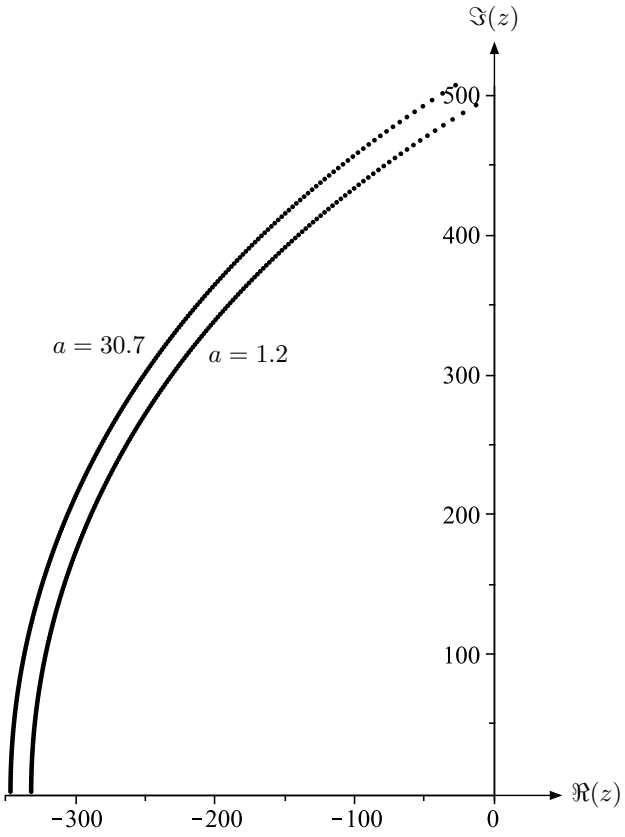

FIG. 4.2. *Zeros in the second quadrant obtained by the numerical algorithm for* $n = 500$ *and* $a = 1.2,\ 30.7$.

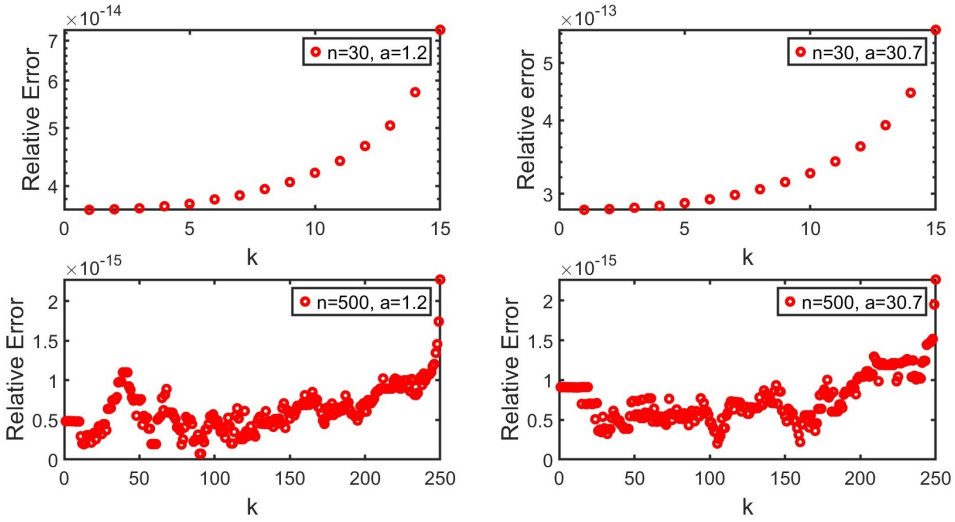

FIG. 4.3. *Relative errors of the computed zeros obtained using the numerical algorithm.*

ETNA
Kent State University and
Johann Radon Institute (RICAM)

TABLE 4.1
Representative CPU times obtained from the execution of our numerical algorithm for $a = 2.3$ and several values of n.

n	CPU time (s)
30	2.8×10^{-3}
200	5.9×10^{-3}
500	1.1×10^{-2}
1000	1.9×10^{-2}
2000	3.7×10^{-2}

factor of 10, despite the number of zeros increasing by a much larger factor.

The good efficiency of our numerical method can also be verified by comparison with Pasquini's method [19] for computing the zeros of generalized Bessel polynomials. Pasquini's algorithm is based on the use of Newton's method to solve a nonlinear system of equations satisfied by the zeros. A key point in the implementation is the use of a good starting point. In Pasquini's paper, the possibility of computing the zeros by solving a related spectral problem is also discussed. However, it is pointed out that reformulating the problem as an eigenvalue computation introduces intrinsic ill-conditioning, whereas the nonlinear formulation derived from the differential equation preserves the mathematical structure and numerical stability.

Using the implementation of Pasquini's method employed in [14], we found that, for example, when $n = 500$, the computational time required by Pasquini's method is 40 times larger than that of our method. For $n = 1000$, this time difference increases to a factor of 140, and for $n = 2000$, to a factor of 539. In all cases, we have taken $a = 1.01$, although similar timing results are obtained for other values of a.

These observations provide clear evidence of the efficiency of the algorithm developed for computing the zeros.

Acknowledgements. We thank the reviewer for his/her useful comments. We also thank the authors of [14] for providing the MATLAB implementation of Pasquini's method.

REFERENCES

[1] S. BOCHNER, *Über Sturm-Liouvillesche polynomsysteme*, Math. Z., 29 (1929), pp. 730–736.
[2] C. CARIMALO, *Maximally flat group delay of Bessel polynomials*, Circuits Systems Signal Process., 37 (2018), pp. 5174–5177.
[3] A. CARPENTER, *Asymptotics for the zeros of the generalized Bessel polynomials*, Numer. Math., 62 (1992), p. 465–482.
[4] M. G. DE BRUIN, E. B. SAFF, AND R. S. VARGA, *On the zeros of generalized Bessel polynomials. I*, Nederl. Akad. Wetensch. Indag. Math., 43 (1981), pp. 1–13.
[5] ———, *On the zeros of generalized Bessel polynomials. II*, Nederl. Akad. Wetensch. Indag. Math., 43 (1981), pp. 14–25.
[6] F. W. J. OLVER, A. B. OLDE DAALHUIS, D. W. LOZIER, B. I. SCHNEIDER, R. F. BOISVERT, C. W. CLARK, B. R. MILLER, B. V. SAUNDERS, H. S. COHL, AND M. A. MCCLAIN, eds., *NIST Digital Library of Mathematical Functions*. Release 1.1.6 of 2022-06-30. https://dlmf.nist.gov/
[7] T. M. DUNSTER, *Uniform asymptotic expansions for the reverse generalized Bessel polynomials, and related functions*, SIAM J. Math. Anal., 32 (2001), pp. 987–1013.
[8] ———, *Uniform asymptotic expansions for the zeros of Bessel functions*, SIAM J. Math. Anal., 56 (2024), pp. 6521–6550.
[9] ———, *Simplified Airy function asymptotic expansions for reverse generalised Bessel polynomials*, J. Classical Anal., 28 (2026), pp. 1–21. DOI: 10.7153/jca-2026-28-01
[10] T. M. DUNSTER, A. GIL, D. RUIZ-ANTOLIN, AND J. SEGURA, *Computation of the reverse generalized Bessel polynomials and their zeros*, Comput. Math. Methods, 3 (2021), Paper No. e1198, 12 pages.

ETNA
Kent State University and
Johann Radon Institute (RICAM)

[11] I. M. FILANOVSKY, *Enhancing amplifiers/filters bandwidth by transfer function zeroes*, in 2015 IEEE International Symposium on Circuits and Systems (ISCAS), IEEE Conference Proceedings, Los Alamitos, 2015, pp. 141–144.
[12] E. GROSSWALD, *Bessel Polynomials*, Springer, Berlin, 1978.
[13] J. JOHNSON, D. JOHNSON, P. BOUDRA, AND V. STOKES, *Filters using Bessel-type polynomials*, IEEE Trans. Circuits Syst., 23 (1976), pp. 96–99.
[14] D. KONG, J. SHEN, L. WANG, AND S. XIANG, *Eigenvalue analysis and applications of the Legendre dual-Petrov-Galerkin methods for initial value problems*, Adv. Comput. Math., 50 (2024), Paper No. 97, 36 pages.
[15] H. KRALL AND O. FRINK, *A new class of orthogonal polynomials: the Bessel polynomials*, Trans. Amer. Math. Soc., 65 (1949), pp. 100–115.
[16] A. B. J. KUIJLAARS AND K. T.-R. MCLAUGHLIN, *Asymptotic zero behavior of Laguerre polynomials with negative parameter*, Constr. Approx., 20 (2004), pp. 497–523.
[17] J. MARTINEZ, *Transfer functions of generalized Bessel polynomials*, IEEE Trans. Circuits Syst., CAS-2 (1977), pp. 325–328.
[18] F. W. J. OLVER, *Asymptotics and Special Functions*, AK Peters, Wellesley, 1997.
[19] L. PASQUINI, *Accurate computation of the zeros of the generalized Bessel polynomials*, Numer. Math., 86 (2000), pp. 507–538.
[20] V. ROMANOWSKY, *Sur quelques classes nouvelles des polynomes orthogonaux*, C. R. Acad. Sci. Paris, 188 (1929), pp. 1023–1025.
[21] J. SEGURA, *Computing the complex zeros of special functions*, Numer. Math., 124 (2013), pp. 723–752.